Test of the proton-neutron interacting boson-fermion model in the region around $A = 190$

J. M. Arias, C. E. Alonso, and M. Lozano
Departamento de Física Atómica y Nuclear, Facultad de Física, 41012 Sevilla, Spain
(Received 11 February 1985)

We present systematic calculations on nuclei in the region around $A = 190$ within the framework of the proton-neutron interacting boson-fermion model. Energy levels and electromagnetic properties of both positive and negative parity states in odd proton ($_{77}$Ir,$_{79}$Au) and odd neutron ($_{78}$Pt) nuclei are compared with experimental data. A general good agreement is obtained with a few adjustable parameters.

I. INTRODUCTION

During the last decade a considerable amount of experimental information on collective excited states of odd-A nuclei has been obtained with new or improved techniques. In particular, the nuclear region around $A = 190$ has been extensively explored via complementary on-line and in-beam γ-ray spectroscopy experiments (see, e.g., Refs. 1–8). This is a very complex region where nuclei display a smooth transition from well-deformed prolate to weakly deformed oblate shapes through soft fluctuating triaxial forms, including various kinds of shape coexistence. Due to these original characteristics, the description of some nuclei around $A = 190$ has been undertaken, in a geometrical approach, by several models, such as the particle-vibration coupling model,[9] the triaxial rotor-plus-particle model,[10] the variable moment of inertia (VMI) model,[11] or the particle-plus-γ soft rotor model.[12]

As an alternative approach to nuclear structure Iachello and Scholten[13] have extended the interacting boson model (IBA) (Refs. 14–16) to odd-A nuclei. This extension has been called the interacting boson-fermion approximation model (IBFA). In the IBFA the collective states in odd-even nuclei are described in terms of a mixed system of interacting bosons and a single fermion. A large variety of odd-A nuclei have been described with a version of this model[17–21] (IBFA-1) in which no distinction is made between neutron and proton degrees of freedom. In order to get a more realistic description of nuclei, the next step in the development of the IBFA model is to include these degrees of freedom explicitly. This new model is called the proton-neutron interacting boson-fermion approximation model[22] or alternatively IBFA-2.

An interesting aspect of IBFA-2 is that it allows one to study proton-neutron effects in odd-A nuclei. This can be done by applying the model simultaneously to a chain of odd-proton and odd-neutron isotopes which have the same even-even core nuclei. The possible differences in the energy spectra between two odd-A nuclei with a common core nucleus can then be ascribed to the difference in coupling between the odd-proton and the odd-neutron to the core.

In IBFA-2 the interaction between the core, described in terms of IBA-2,[23,24] and the single fermion is described essentially by two terms: (i) a quadrupole-quadrupole interaction between the single proton (neutron) and the neutron-bosons (proton-bosons) of the core, and (ii) an exchange term[25,26] which takes into account the fact that the single fermion is coupled to bosons which are built out of fermions that may occupy the same single-particle levels as the single fermion.

In this paper we present a study within the IBFA-2 for both positive and negative parity states of odd-neutron platinum isotopes, odd-proton iridium isotopes, and the unique parity $\pi h_{9/2}$ level system in odd-proton gold isotopes. From an algebraic point of view, in the transitional region around $A = 190$ the even-even nuclei (Os-Pt) present[27] a smooth and continuous change from SU(3) to O(6) limits[15] of IBA. Therefore we describe the overall trends of the energy spectra and electromagnetic properties of each family rather than giving a detailed description of each nucleus. In this way we are able to study a large amount of experimental information with only a few parameters, and we obtain a comprehensive view of this nuclear region.

The aim of this work is to test the ability of the model to reproduce the experiments and to know at which extent IBFA-2 represents an advantage with respect to IBFA-1.

In Sec. II we briefly present the IBFA-2 Hamiltonian. We have performed single level calculations for the description of the unique parity level systems ($\pi h_{11/2}$ in $_{77}$Ir, $\nu i_{13/2}$ in $_{78}$Pt, and $\pi h_{9/2}$ in $_{79}$Au), and multilevel calculations for the study of positive parity levels in Ir isotopes and negative parity levels in Pt isotopes. The results of these energy spectra calculations are presented in Sec. III. Section IV is dedicated to the discussion of electromagnetic properties, and finally in Sec. V we present the main conclusions of this work.

II. THE IBFA-2 HAMILTONIAN

In the IBFA-2 model the Hamiltonian is written as

$$H = H_B + H_F + V_{BF} \tag{1}$$

where H_B is the IBA-2 Hamiltonian, H_F is the fermion Hamiltonian describing the single-particle degrees of freedom, and V_{BF} is the interaction between the boson and fermion degrees of freedom. The even-even core nucleus Hamiltonian H_B is written as[27,28]

$$H_B=\varepsilon_\pi\hat{n}_{d,\pi}+\varepsilon_\nu\hat{n}_{d,\nu}+\kappa Q_\pi^{(2)}\cdot Q_\nu^{(2)} + V_{\pi\pi}+V_{\nu\nu}+M_{\pi\nu}\ , \tag{2}$$

where the first two terms represent the single boson energies for protons (π) and neutrons (ν), respectively: $\varepsilon_\pi(\nu)$ is the energy difference between $d_{\pi(\nu)}$ and $s_{\pi(\nu)}$ bosons, and $\hat{n}_{d,\pi(\nu)}$ is the number of proton (neutron) d bosons ($\rho=\pi,\nu$ hereafter)

$$\hat{n}_{d,\rho}=\sum_m d^\dagger_{\rho,m}d_{\rho,m}\ . \tag{3}$$

The quadrupole operator of the quadrupole-quadrupole interaction between neutron and proton bosons with strength κ is expressed as

$$Q^{(2)}_{\rho_\mu}=(s^\dagger_\rho\tilde{d}_\rho+d^\dagger_\rho\tilde{s}_\rho)^{(2)}_\mu+\chi_\rho(d^\dagger_\rho\tilde{d}_\rho)^{(2)}_\mu\ . \tag{4}$$

The terms $V_{\pi\pi}$ and $V_{\nu\nu}$ represent d-boson conserving residual proton-proton and neutron-neutron interactions, respectively.

$$V_{\rho\rho}=\sum_{L=0,2,4}\tfrac{1}{2}C^\rho_L(d^\dagger_\rho d^\dagger_\rho)^{(L)}(\tilde{d}_\rho\tilde{d}_\rho)^{(L)}+\kappa_\rho Q^{(2)}_\rho\cdot Q^{(2)}_\rho\ . \tag{5}$$

The Majorana term included in (2) is given by:

$$M_{\pi\nu}=\xi_2(s^\dagger_\pi d^\dagger_\nu-d^\dagger_\pi s^\dagger_\nu)^{(2)}(\tilde{s}_\pi\tilde{d}_\nu-\tilde{d}_\pi\tilde{s}_\nu)^{(2)} -2\sum_{\lambda=1,3}\xi_\lambda(d^\dagger_\pi d^\dagger_\nu)^{(\lambda)}(\tilde{d}_\pi\tilde{d}_\nu)^{(\lambda)}\ . \tag{6}$$

The fermion Hamiltonian in (1) contains only one-body terms

$$H_F=\left[\sum_{jm}E_j a^\dagger_{jm}a_{jm}\right]_\rho\ , \tag{7}$$

where the coefficients E_j are the single-particle energies in the presence of N pairs and $a^\dagger_{jm}(a_{jm})$ is the creation (destruction) operator of a fermion in the state $|jm\rangle$.

The interaction between the core and the odd nucleon must be expressed by many different terms, especially because one has to take into account the effects of the Pauli principle due to the composite character of the bosons. Thus the number of parameters involved in such a general expression of V_{BF} is so high that a phenomenological treatment would not be possible. In several microscopic approaches[19,26] the importance of the various terms in the boson-fermion interaction has been studied. Based on those approaches, Scholten and Dieperink[25] have derived in the generalized seniority scheme,[29] using the number operator approximation[30,31] and the mapping procedure of Ref. 32, the following expressions:

$$V_{BF}=\Gamma_\nu Q^{(2)}_\pi\cdot q^{(2)}_\nu+\Lambda_\nu F_{\pi\nu}+A_\nu\hat{n}_{d,\pi}\hat{n}_\nu \tag{8}$$

for odd neutron nuclei, and

$$V_{BF}=\Gamma_\pi Q^{(2)}_\nu\cdot q^{(2)}_\pi+\Lambda_\nu F_{\nu\pi}+A_\pi\hat{n}_{d,\nu}\hat{n}_\pi \tag{9}$$

for odd proton nuclei. The essential assumption on which these expressions are based, is that since in even-even nuclei the proton-neutron quadrupole-quadrupole interaction plays a dominant role in the description of low-lying collective states, it is expected that the most important terms in the boson-fermion interaction also arise from a quadrupole force. Thus the first term in Eqs. (8) and (9) represents the quadrupole-quadrupole interaction between bosons and fermions with

$$q^{(2)}_\rho=\left[\sum_{j,j'}(u_ju_{j'}-v_jv_{j'})Q_{jj'}(a^\dagger_j\tilde{a}_{j'})^{(2)}\right]_\rho\ , \tag{10}$$

where we have introduced the shell model occupation probabilities, which in the generalized seniority scheme are given by

$$v_j=\left[\alpha_j^2N/\sum_{j'}\alpha^2_{j'}(j'+\tfrac{1}{2})\right]^{1/2}\ , \qquad u_j=(1-v_j^2)^{1/2}\ . \tag{11}$$

Here the α_j's are the structure constants of the S pairs creation operators and N the number of pairs. The coefficients $Q_{jj'}$ are the reduced matrix elements of the spherical harmonics of rank two

$$Q_{jj'}=\langle l,\tfrac{1}{2},j||Y^{(2)}||l',\tfrac{1}{2},j'\rangle\ . \tag{12}$$

The second term in Eqs. (8) and (9) is an exchange term, which takes into account the effect of the Pauli principle and arises from the interpretation of the bosons as correlated pairs:

$$F_{\pi\nu}=-[(s^\dagger\tilde{d})^{(2)}]_\pi\left\{\sum_{j,j',j''}\left[\frac{10}{N(2j+1)}\right]^{1/2}Q_{jj'}\beta_{j''j}(u_jv_{j'}+v_ju_{j'}):[(d^\dagger\tilde{a}_{j''})^{(j)}(a^\dagger_{j'}\tilde{s})^{(j')}]^{(2)}:\right\}_\nu+\text{H.c.}\ , \tag{13}$$

where the coefficients $\beta_{jj'}$ are related to the structure of the D pairs[19] and are given by:

$$\beta_{jj'}=(u_jv_{j'}+v_ju_{j'})Q_{jj'}\ . \tag{14}$$

$F_{\nu\pi}$ can be expressed from Eq. (13) by interchanging the indices π and ν. The third term in Eqs. (8) and (9) represents a monopole-monopole interaction with

$$\hat{n}_\rho=\left[\sum_{j,m}a^\dagger_{jm}a_{jm}\right]_\rho\ . \tag{15}$$

In the actual calculations the occupation probabilities and the single-particle energies are calculated using the Bardeen-Cooper-Schrieffer (BCS) approximation rather than the full generalized seniority scheme

$$E_j=[(\varepsilon_j-\lambda)^{(2)}+\Delta^2]^{1/2}\ , \qquad v_j=\{\tfrac{1}{2}[1-(\varepsilon_j-\lambda)/E_j]\}^{1/2}\ , \qquad u_j=(1-v_j^2)^{1/2}\ , \tag{16}$$

and

This core-particle interaction provides a simple framework for phenomenological calculations, thus the spectra of odd-even nuclei can be obtained in terms of three parameters, namely the strengths of the quadrupole, the exchange, and the monopole terms, $\Gamma_\rho, \Lambda_\rho, A_\rho$ in Eqs. (8) and (9). For the present calculations we have used the computer code ODDPAR written by Visscher and Bijker.[22,23]

III. THE ENERGY SPECTRA

In the region around $A=190$ one finds bands built on the unique parity, high-j, single-particle levels ($\pi h_{11/2}$) in the major shell 50-82 for protons and ($\nu i_{13/2}$) in the 82-126 shell for neutrons. These are the simplest situations to be described. There are other more complicated configurations involving four or five single-particle levels. The study of both situations provides a stringent test of the IBFA-2 model. We have used the IBA-2 parameters for the even-even cores from Ref. 27. The odd proton (neutron) coupled to these cores is allowed to occupy the single-particle levels displayed in Figs. 1(a) and (b). In Tables I—III we present the results of the BCS calculation.

A. Ir isotopes

The $^{A}_{77}$Ir isotopes are described in the IBFA-2 model by coupling the odd hole proton to the corresponding even-even $^{A+1}_{78}$Pt IBA-2 core nucleus. For the negative parity states there is only one single-particle level available in the major shell 50-82: $1h_{11/2}$. For the positive parity states there are four single-particle levels: $3s_{1/2}$, $2d_{3/2}$, $2d_{5/2}$, and $1g_{7/2}$. Besides these configurations, there also exists an intruder $1h_{9/2}$ negative parity system of levels which may be described by coupling the odd proton to the corresponding even-even $^{A-1}_{76}$Os core. In our calculations we do not consider the mixing between these $h_{11/2}$ and $h_{9/2}$ bands, because the effect of the coupling is known to be small.[33]

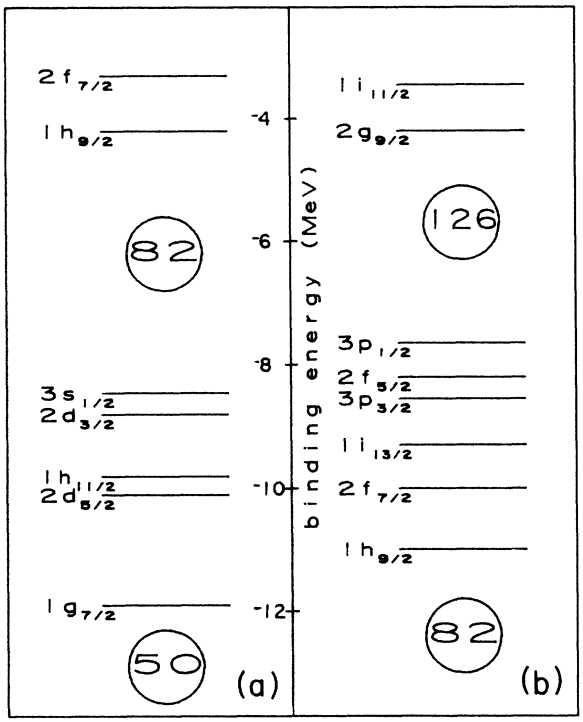

FIG. 1. Single particle levels (Ref. 35) used in this work.

1. The $\pi h_{11/2}$ system of levels

The experimental[6,7,33–35] $\pi h_{11/2}$ system of levels includes two strongly coupled rotational bands based on the $\frac{11}{2}^-$ isomeric state and the $\frac{7}{2}^-$ level. In Fig. 2 we display the experimental information of these levels along with the theoretical IBFA-2 results. The parameters used in the calculations are presented in Table IV. In Fig. 2 we see that the IBFA-2 results reproduce the general trends of the spectra. In particular, the lowering of the $J=j\pm1$ levels and the raising of the $J=j\pm2$ levels for decreasing

TABLE I. BCS parameters for Ir isotopes (E_j in MeV). The unperturbed single-particle energies used are given in Fig. 1.

A		$1g_{7/2}$	$2d_{5/2}$	$1h_{11/2}$	$2d_{3/2}$	$3s_{1/2}$	$1h_{9/2}$
185	E_j	3.310	1.646	1.379	0.885	0.926	4.596
	v_j^2	0.982	0.922	0.884	0.539	0.349	0.009
187	E_j	3.306	1.642	1.374	0.880	0.922	4.597
	v_j^2	0.982	0.923	0.885	0.538	0.347	0.009
189	E_j	3.303	1.637	1.369	0.875	0.918	4.598
	v_j^2	0.982	0.923	0.885	0.537	0.345	0.009
191	E_j	3.299	1.633	1.365	0.871	0.915	4.600
	v_j^2	0.982	0.923	0.886	0.536	0.343	0.009
193	E_j	3.296	1.629	1.360	0.866	0.911	4.601
	v_j^2	0.983	0.924	0.886	0.535	0.341	0.009
195	E_j	3.293	1.624	1.356	0.861	0.907	4.602
	v_j^2	0.983	0.924	0.887	0.534	0.339	0.009

TABLE II. BCS parameters for the single j-orbit calculations in Pt and Au (E_j in MeV). The unperturbed single-particle energies are given in Fig. 1.

	Band		$A=185$	$A=187$	$A=189$	$A=191$	$A=193$	$A=195$
Pt	$i_{13/2}$	E_j	0.883	0.897	0.942	1.020	1.130	1.269
		v_j^2	0.515	0.604	0.688	0.762	0.822	0.868
Au	$h_{9/2}$	E_j	4.193	4.196	4.198	4.201	4.203	4.205
		v_j^2	0.011	0.011	0.011	0.011	0.011	0.011

A. As in the IBFA-1 calculation[17] the strength of the exchange force had to be increased with decreasing value of A in order to reproduce the trend of the $J=j-1$ state. As in IBFA-1 the striking overall behavior of the $\frac{7}{2}_1$ level is reproduced but the theoretical values are too high.

In our calculation the monopole-monopole term is not necessary. Hence we describe the features of the spectra with only two parameters, one of them fixed and the other varying smoothly from isotope to isotope.

In Fig. 3 we present a detailed comparison of the experimental and calculated spectrum of the ^{187}Ir isotope, which shows the characteristics of the SU(3)-plus-particle coupling scheme. For the heavier iridium isotopes we see (Fig. 2) that their spectra are closer to an O(6)-plus-particle scheme.

2. The $\pi h_{9/2}$ system of levels

As it is well known,[6,7,33,36] along with the $\pi h_{11/2}$ negative parity band, the Ir isotopes present a $\frac{9}{2}^-$ system of levels with the character of the decoupled band. This intruder band is described in IBFA-2 by coupling a proton to the corresponding even-even $_{76}$Os IBA-2 core nucleus [$^{A}_{76}\mathrm{Os}\times(\pi h_{9/2})\rightarrow{}^{A+1}_{77}\mathrm{Ir}$]. Figure 4 displays the experimental and calculated levels for the $h_{9/2}$ system in the Ir isotopes. In Fig. 5 a more detailed spectrum of a single isotope is shown. The orbital $h_{9/2}$ is far away from the active major shell 50-82 so its occupancy is practically null and thus the exchange term is unimportant. Hence in this calculation we only need one parameter, the strength of the quadrupole term which was fixed to $\Gamma_\pi=0.3$ MeV for all the isotopes. Figure 4 shows that the calculation reproduces the experimentally observed features. The spectra of the $h_{9/2}$ band of the $_{77}$Ir isotopes look more like a SU(3)-plus-particle scheme. This can be explained by the fact that the even-even $_{76}$Os isotopes have a larger number of proton bosons than the corresponding Pt isotopes. Moreover, one must note that the available experimental information on this band is mainly referred to the lighter isotopes which are expected to have spectra close to the SU(3)-plus-particle limit.

TABLE III. BCS parameters for the negative-parity state calculation (E_j in MeV) in ^{195}Pt. The unperturbed single-particle energies are given in Fig. 1.

	$1h_{9/2}$	$2f_{7/2}$	$3p_{3/2}$	$3f_{5/2}$	$3p_{1/2}$
E_j	2.894	1.855	0.881	0.870	1.112
v_j^2	0.977	0.943	0.610	0.422	0.183

3. Positive parity states

The positive parity states are described by coupling the $1g_{7/2}$, $2d_{5/2}$, $2d_{3/2}$, and $3s_{1/2}$ shell model orbits to the even-even core nuclei. In Fig. 6 the energy spectra[6,7,33,37,38] are displayed. As one can see, the systematics of these low-energy levels shows a smooth variation from ^{195}Ir to ^{185}Ir. The calculation reproduces the general trends of the experimental values. The smoothness of the variation of the energy levels is well described. The Ir nuclei have 77 protons and when one moves from isotope to isotope the occupation probabilities of the single-particle levels (v_j) and the quasiparticle energies (E_j) remain nearly constant. Therefore the effect of the exchange interaction is almost the same for all the isotopes and the spectra are determined by the quadrupole interaction. The latter increases when N decrease determines the transition from an O(6)-plus-particle to a SU(3)-plus-particle scheme. The three parameters needed in the calculation were fixed for all the isotopes: $\Gamma_\pi=0.1$ MeV, $\Lambda_\pi=0.15$ MeV, and $A_\pi=-0.2$ MeV. Figure 7 displays the experimental and calculated spectra of ^{191}Ir in detail.

B. Pt isotopes

In the framework of the IBFA-2 model the odd-A $_{78}$Pt isotopes are described by coupling the odd hole neutron to the corresponding $^{A+1}_{78}$Pt core nucleus described by the IBA-2 model. There is a single-particle level ($\nu i_{13/2}$) of positive parity available to the odd neutron in the major shell 82-126 and five of negative parity: $1h_{9/2}$, $2f_{7/2}$, $3p_{3/2}$, $2f_{5/2}$, and $3p_{1/2}$. Tables II and III display the results of a simple BCS calculation for the occupation probabilities and quasiparticle energies.

1. Positive parity states

In Fig. 8 the experimental data[3,4,8,35,39,41] of the $\nu i_{13/2}$ band are presented along with the IBFA-2 results. The parameters used in these calculations are collected in Table IV. A striking feature of these spectra is the existence in the heavier isotopes of well-decoupled $\nu i_{13/2}$ bands and the presence at very low energy of the $\frac{11}{2}^+$ level. This is a consequence of the γ softness of the core nucleus [O(6) limit in IBA (Ref. 15)]. From the heavier to the lighter isotopes there is a crossing between the $J=j$ and $J=j-1$ levels leading to a strong coupling scheme [SU(3)-plus-particle limit in IBFA]. This behavior is qualitatively reproduced by the calculation. The lowering of the unfavored levels ($\frac{11}{2}, \frac{15}{2}, \ldots$) is ascribed to the lo-

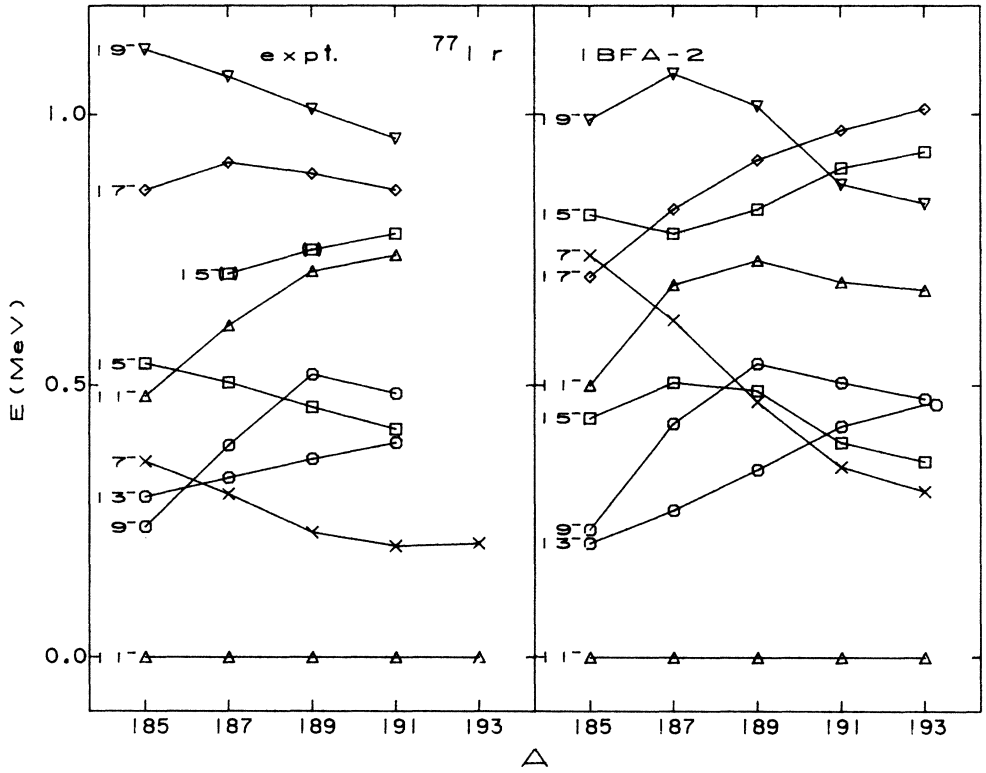

FIG. 2. Experimental (Refs. 6, 7, and 33–35) and IBFA-2 systematics of the $\pi h_{11/2}$ band in Ir isotopes. The state $J^p=\frac{11}{2}^-$ is taken as zero of energy. Numbers at the left of the curves are twice the spin of the level.

cation of the Fermi level in the Nilsson model. In IBFA-2 this feature is due (apart from the effect of the core) to the exchange term which is related to the occupation probabilities of the level. Thus this term is zero when the level is full or empty and gets its maximum value when it is occupied at fifty percent. The calculation also reproduces qualitatively the lowering of the $J=j-2$ level with respect to the $J=\frac{13}{2}^+$ level. However, quantitatively the $J=\frac{9}{2}^+$ calculated level is much higher than the experimental value. There exists some evidence[3,4,42] that the pickup reactions from $\frac{9}{2}^+$ states have a strength greater than that expected from a Nilsson study for the $\frac{9}{2}^+$ [624] which indicates the presence of an intruder $\frac{9}{2}^+$ band. This intruder band would come from the $2g_{9/2}$ single-particle orbital. Figure 9 presents a more detailed comparison between experiment and theory for a single nucleus.

2. *Negative parity states*

The situation in odd-A Pt isotopes for the negative parity states is quite complex due to the large density of states below 1 MeV. Moreover, a study of the systematics of the energy levels is impossible since there are a lot of states with uncertain or no spin assignment. A more concluding experimental investigation in this region would be very desirable. Nevertheless and for the sake of complete-

TABLE IV. Boson-fermion interaction parameters used in the calculations.

	Calculation	A	ρ	Γ_ρ (MeV)	Λ_ρ (MeV)	A_ρ (MeV)
Ir	$h_{11/2}$ band	185	π	0.40	0.80	0.0
		187		0.40	0.50	0.0
		189		0.40	0.25	0.0
		191,193		0.40	0.20	0.0
	$h_{9/2}$ band	185–189		0.30	0.00	0.0
	positive-parity states	185–195		0.10	0.15	−0.2
Pt	$i_{13/2}$ band	185–195	ν	0.30	0.90	−0.3
	negative-parity states	195		0.65	0.65	−0.5
Au	$h_{9/2}$ band	185–197	π	0.30	0.00	−0.1

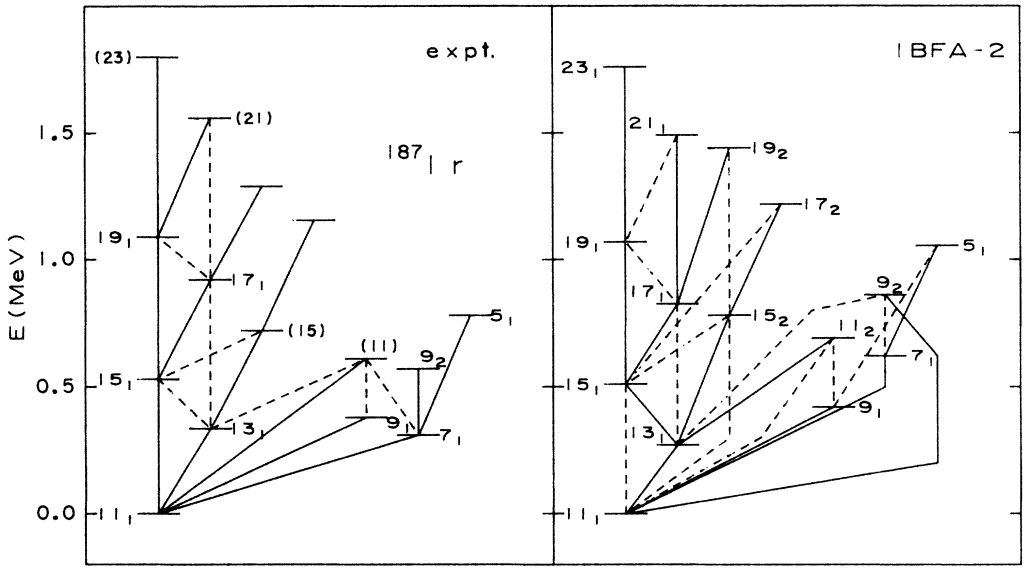

FIG. 3. Detailed comparison between experimental (Ref. 33) and IBFA-2 spectra for the $h_{11/2}$ system of levels in ^{187}Ir. The lines between levels denote total transition probabilities: solid for the strongest one and broken for weaker ones. Calculated transition probabilities are based on $B(E2)$ and $B(M1)$ values. Numbers in the figure are twice the spin.

ness, we have calculated the energy spectrum of ^{195}Pt for which there exists a rather complete study.[41] In this calculation five single-particle levels in the major shell 82-126 are involved ($1h_{9/2}$, $2f_{7/2}$, $3p_{3/2}$, $2f_{5/2}$, and $3p_{1/2}$). In Fig. 10 the experimental and the theoretical levels are displayed. The parameters of this calculation are presented in Table IV. We note that the calculation reproduces only the number (11) of $J=\frac{1}{2}^-$, $\frac{3}{2}^-$ states below 1 MeV. All the calculated levels below 1 MeV are plotted in Fig. 10.

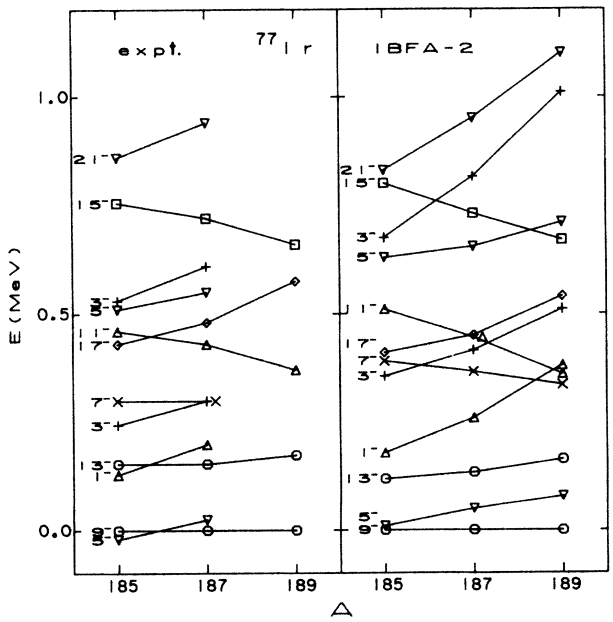

FIG. 4. Experimental (Refs. 6, 7, and 33–36) and IBFA-2 systematics of the $\pi h_{9/2}$ intruder band in Ir isotopes. The state $J^p=\frac{9}{2}^-$ is taken as zero of energy. Numbers at the left of the curves are twice the spin of the level.

C. The intruder $\pi h_{9/2}$ band in gold isotopes

Odd-A gold isotopes present, besides the $\pi h_{11/2}$ band, an intruder $\pi h_{9/2}$ system of levels. This band is described in the proton-neutron IBFA model by coupling the odd proton in the $1h_{9/2}$ single-particle level with the corresponding Pt core nucleus: $^{A}_{78}\mathrm{Pt}\times\pi h_{9/2}\rightarrow{}^{A+1}_{79}\mathrm{Au}$. This is a very simple case since the $1h_{9/2}$ proton level is almost empty and then the effect of the exchange term is practically negligible. So in this chain of isotopes the behavior of the energy spectra is basically due to the quadrupole interaction. In Fig. 11 we present the experimental[43–45] and the calculated spectra. The parameters used in the calculation are given in Table IV. The main features of the spectra are well reproduced by the calculations. The sudden lowering in energy of the states $J=\frac{5}{2}^-$, $\frac{7}{2}^-$ when one goes towards the lighter isotopes is a clear evidence of the increasing in the quadrupole interaction yielding a strong coupling scheme [SU(3)-plus-particle]. On the other hand, the behavior of the $J=\frac{11}{2}^-$ state, at an energy

TABLE V. Quadrupole moments (in e b) for ^{191}Ir and ^{193}Ir.

Nucleus	J^p	Expt.	IBFA-2
^{191}Ir	$\frac{3}{2}^+_1$	$+0.81(21)^a$	0.16
^{193}Ir	$\frac{3}{2}^+_1$	$+0.73(19)^b$	0.07

[a]Reference 47.
[b]Reference 48.

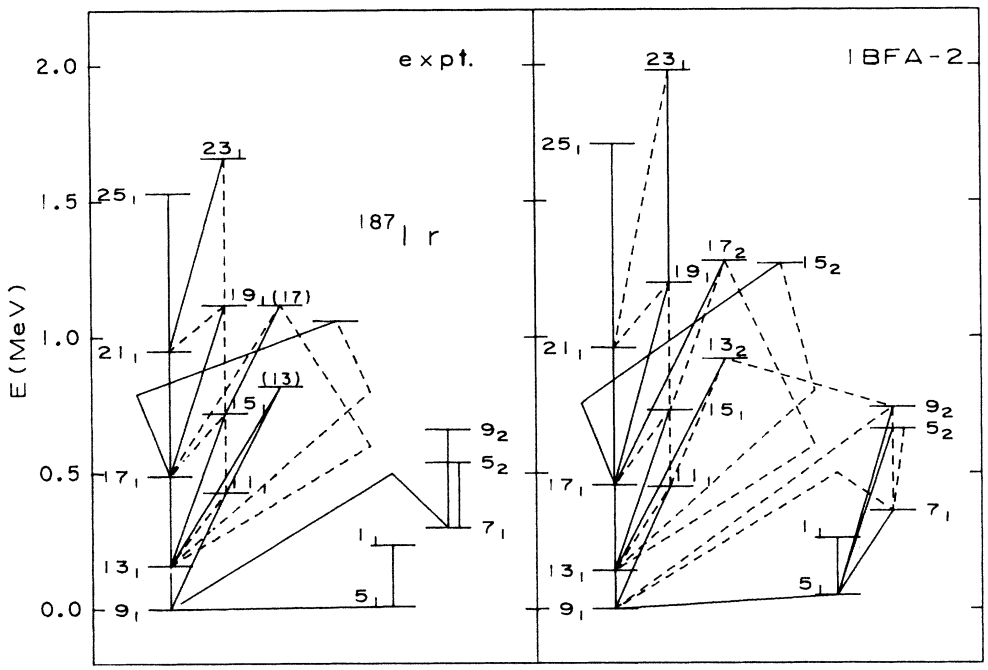

FIG. 5. Same as Fig. 3 but for the $\pi h_{9/2}$ intruder band (Refs. 33 and 53) in ^{187}Ir.

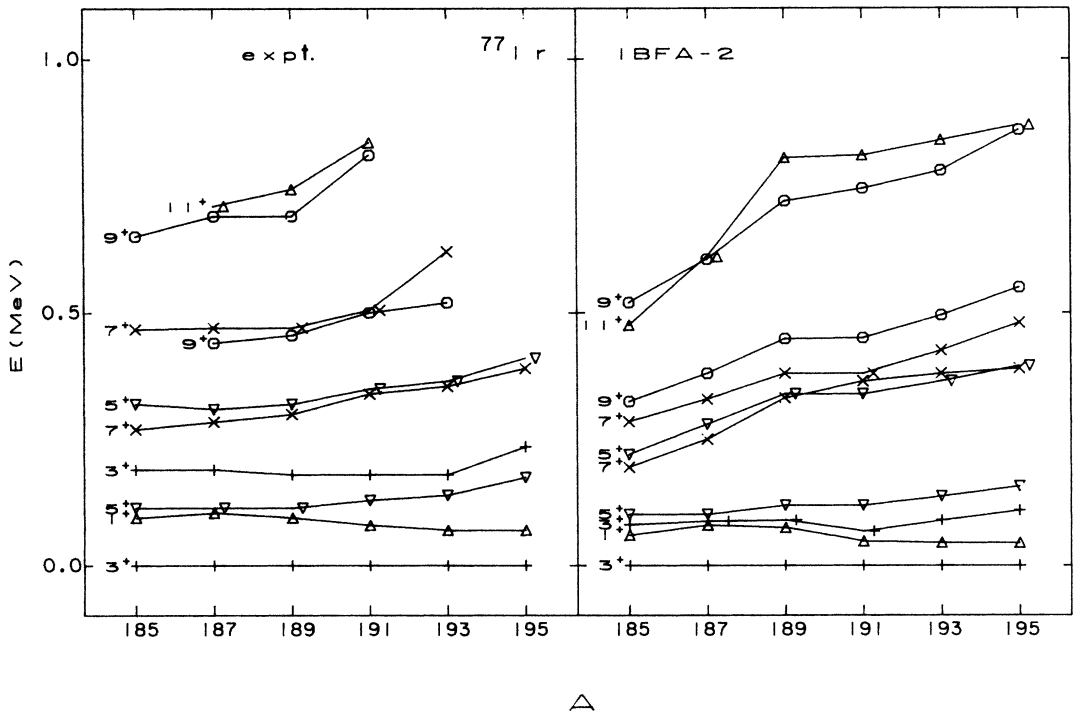

FIG. 6. Experimental (Refs. 6, 7, 33, 37, and 38) and IBFA-2 systematics of the positive parity states in Ir isotopes. The state $J^p=\frac{3}{2}^+$ is taken as zero of energy. Numbers at the left of the curves are twice the spin of the level.

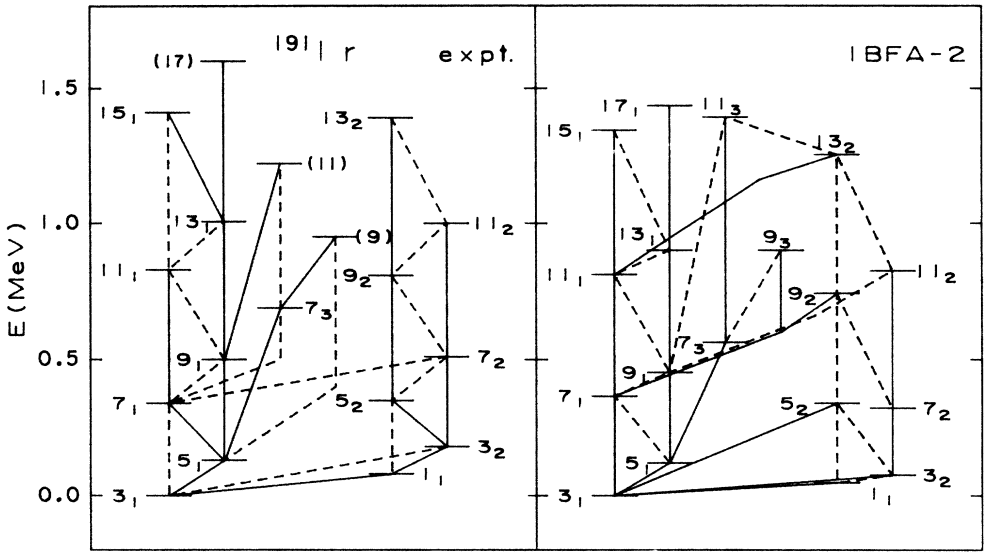

FIG. 7. Same as Fig. 3 but for the positive parity states (Ref. 34) in ^{191}Ir.

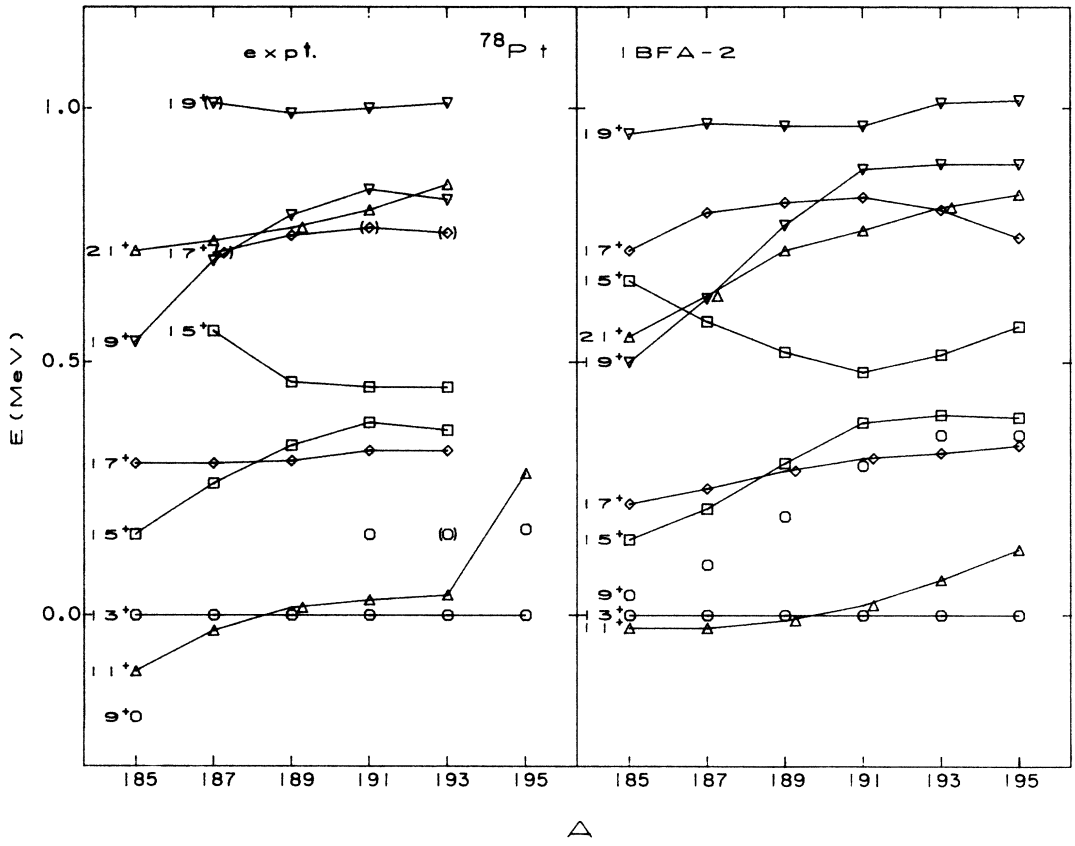

FIG. 8. Experimental (Refs. 3, 4, 8, 35, and 39–41) and IBFA-2 systematics of the $\nu i_{13/2}$ band in Pt isotopes. The state $J^p = \frac{13}{2}^+$ is taken as zero of energy. Numbers at the left of the curves are twice the spin of the level.

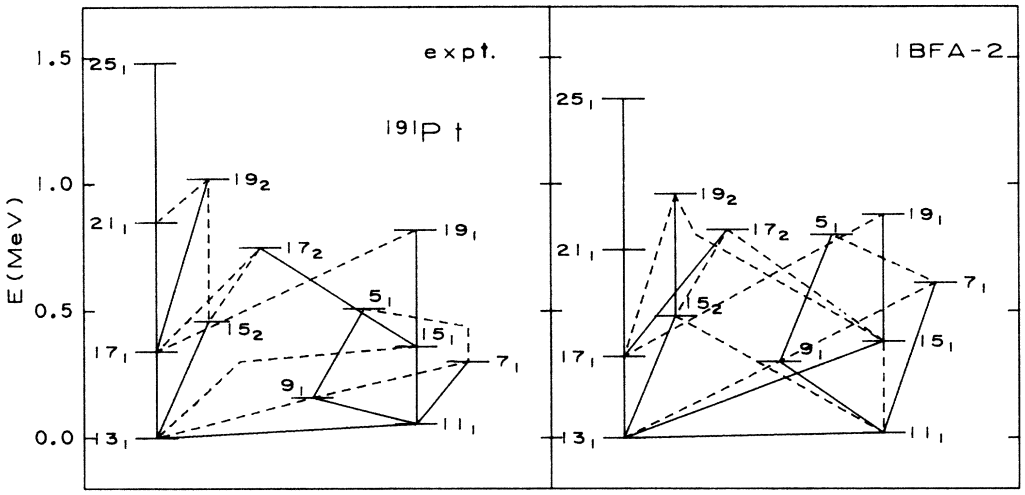

FIG. 9. Same as Fig. 3 but for the $vi_{13/2}$ band (Refs. 3 and 39) in ^{191}Pt.

fairly constant for all the isotopes, indicates that the effect of the γ softness in the core nuclei compensates for the effect of the quadrupole interaction. Other evidence of the transition from the O(6)-plus-particle scheme to the SU(3)-plus-particle scheme when the neutron number decreases is the crossing between the levels $\frac{11}{2}^-$-$\frac{13}{2}^-$ and $\frac{15}{2}^-$-$\frac{17}{2}^-$ which is reproduced by the calculations.

IV. ELECTROMAGNETIC PROPERTIES IN THE IBFA-2

In order to check the wave functions obtained by diagonalizing the Hamiltonian, we have calculated electromagnetic properties. The $E2$ moments and transition probabilities give us an idea of the correctness of the bosonic part of the wave functions because the main contribution to them comes from the bosons. The $M1$ transitions and moments will provide us with information about the fermionic part of the wave functions, since they depend mostly on it.

A. $E2$ transitions and quadrupole moments

We begin by writing the most general form of the one-body $E2$ operator in IBFA-2

$$T(E2)=e_\pi Q_\pi+e_\nu Q_\nu+\sum_{j\le j'} e_F^{(2)} e_{jj'}^{(2)}[(a_j^\dagger \tilde{a}_{j'})^{(2)}+\text{H.c.}] , \tag{17}$$

where Q_π and Q_ν are the bosonic quadrupole operators for protons and neutrons, respectively, and, in general, are given by

$$Q_\rho=\alpha_\rho(s^\dagger \tilde{d}+d^\dagger \tilde{s})_\rho^{(2)}+\bar{\chi}_\rho^{(2)}(d^\dagger \tilde{d})_\rho^{(2)} , \tag{18}$$

e_π (e_ν) is the bosonic effective charge for protons (neutrons), $e_F^{(2)}$ is the fermionic effective charge, and $e_{jj'}^{(2)}$ is written as,[52]

$$e_{jj'}^{(2)}=-\frac{1}{\sqrt{5}}\langle j||Y^{(2)}||j'\rangle(u_j u_{j'}-v_j v_{j'}) . \tag{19}$$

From the matrix elements of $T(E2)$ we can proceed to calculate $B(E2)$'s and quadrupole moments as follows:

$$B(E2;J_i\to J_f)=\frac{1}{2J_i+1}|\langle J_i||T(E2)||J_f\rangle|^2 ,$$
$$Q(J)=\left[\frac{16\pi}{5}\frac{J(2J-1)}{(2J+3)(J+1)}B(E2;J\to J)\right]^{1/2} . \tag{20}$$

B. $M1$ transitions and magnetic moments

For $M1$ transitions the operator in IBFA-2 has the general form

$$T(M1)=\sqrt{3/4\pi}\left\{g_\pi\sqrt{10}(d^\dagger \tilde{d})_\pi^{(1)}+g_\nu\sqrt{10}(d^\dagger \tilde{d})_\nu^{(1)} + \sum_{j\le j'} e_{jj'}^{(1)}[(a_j^\dagger \tilde{a}_{j'})^{(1)}+\text{H.c.}]\right\} , \tag{21}$$

where g_π (g_ν) is the effective g factor for proton (neutron) bosons and

$$e_{jj'}^{(1)}=-\frac{1}{\sqrt{3}}\langle l_j,\tfrac{1}{2},j||g_{l_\rho}\mathbf{l}+g_{s_\rho}\mathbf{s}||l_{j'},\tfrac{1}{2},j'\rangle(u_j u_{j'}+v_j v_{j'}) ; \tag{22}$$

here g_{l_ρ} and g_{s_ρ} are the single particle g factors.

The expressions of $B(M1)$ and magnetic moments from $T(M1)$ are

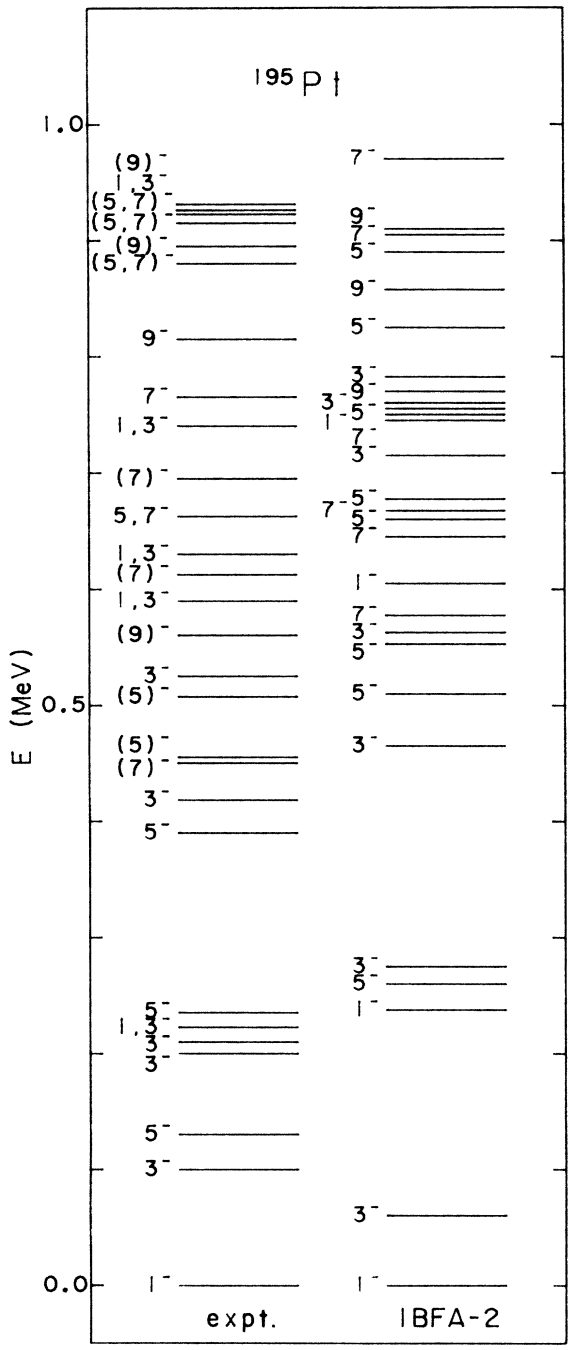

FIG. 10. Comparison between experimental (Ref. 41) and IBFA-2 spectra for the negative parity states in ^{195}Pt.

$$B(M1;J_i \rightarrow J_f)=\frac{1}{2J_i+1}\,|\langle J_i||T(M1)||J_f\rangle|^2\,,$$
$$\mu(J)=\left[\frac{4\pi}{3}\frac{J}{J+1}B(M1;J\rightarrow J)\right]^{1/2}. \tag{23}$$

C. Positive parity states

We have calculated $B(E2)$'s for some transitions between low-lying states in $^{187-193}$Ir, for which there exist experimental data.[37,47–50] The results are presented in Fig. 12. We have chosen $\alpha_\rho=1$ and $\bar{\chi}_\rho^{(2)}=\chi_\rho$, so that the quadrupole operator Q_ρ is the same as the one used for the Hamiltonian, and $e_\pi=e_\nu=e_F^{(2)}=0.17$ e b. The value of the effective charge was taken to be equal for both kinds of bosons and for the odd proton for the sake of simplicity. This value has been taken from Ref. 27.

The agreement between experimental and calculated values is poor. The calculations were performed without any free adjustable parameter. In order to improve the results we tried some adjustment of the single-particle levels. It turns out that the quality of the fits was not better, on average, than that obtained with the energy levels given in Fig. 1.

We have also calculated the quadrupole moments of the ground states of $^{191-193}$Ir. The results are given in Table V. The evaluated quadrupole moments are one order of magnitude smaller than the experimental one.[35,47,48,51] This is probably due to the small value of $\chi_\pi+\chi_\nu$ used in the IBA-2 core calculation, as it is claimed in Ref. 27. This calculation yields very low values for the quadrupole moment of the 2_1^+ states, and the states 2_2^+ and 3_1^+ very high in energy. Moreover, the $\frac{3}{2}^+_1$ state in ^{191}Ir and ^{193}Ir has 92% and 94%, respectively, of $(d_{3/2}\times 0_1^+)^{3/2}$.

Another option can be used for the effective charges by letting e_ν change with the number of neutron bosons, as proposed in Ref. 27. We have verified that this assumption does not improve the results significantly.

As expected, the main contribution to the $E2$ matrix elements is the bosonic one. The fermionic contribution is only larger than 5% in some inhibited transitions.

We have calculated $M1$ reduced transition probabilities between some positive parity states in $^{187-193}$Ir and they are displayed in Table VI. The values of the parameters g_π and g_ν appearing in the $M1$ operator have been taken from Ref. 46. The values used for g_{l_π} and g_{s_π} are 1 and $0.7g_{s_\pi}^{\text{free}}$, respectively.

The agreement between calculated and experimental values[37,47,49] is rough; in general, the weak transitions are calculated to be weak and the strong ones to be strong. Nevertheless, the experimental value of $B(M1;\frac{3}{2}^+_1\rightarrow\frac{1}{2}^+_1)$ in ^{187}Ir is predicted too large. This is due to the composition of the theoretical wave functions: The $\frac{1}{2}^+_1$ state in ^{187}Ir has a strong component (79%) in $(d_{3/2}\times 2_1^+)^{1/2}$ which is connected to the component $(d_{3/2}\times 2_2^+)^{3/2}$ of $\frac{3}{2}^+_1$ ($\sim$1%) by $M1$ transition. In the other isotopes the state $\frac{1}{2}^+_1$ is mainly $(s_{1/2}\times 0_1^+)^{1/2}$ which is not connected to the components of $\frac{3}{2}^+_1$ by $M1$ transitions.

Magnetic moments for ^{191}Ir and ^{193}Ir have also been calculated. We present them in Table VII. If we observe the experimental value of $\mu(\frac{3}{2}^+_1)$ in ^{191,193}Ir, these states seem to be rather pure $d_{3/2}$ [$\mu_\pi^{\text{s.p.}}(d_{3/2})=0.126\ \mu_N$]. In our calculation more than 90% of this state is $(d_{3/2}\times 0_1^+)^{3/2}$, as we mentioned before.

We could expect that the $\frac{1}{2}^+_1$ state was $(s_{1/2}\times 0_1^+)^{1/2}$, basically. If we observe its experimental magnetic moment and compare it with the one predicted by the shell model [$\mu_\pi^{\text{s.p.}}(s_{1/2})=2.79\ \mu_N$], we can see that it must have other components and not be pure. Our calculation gives

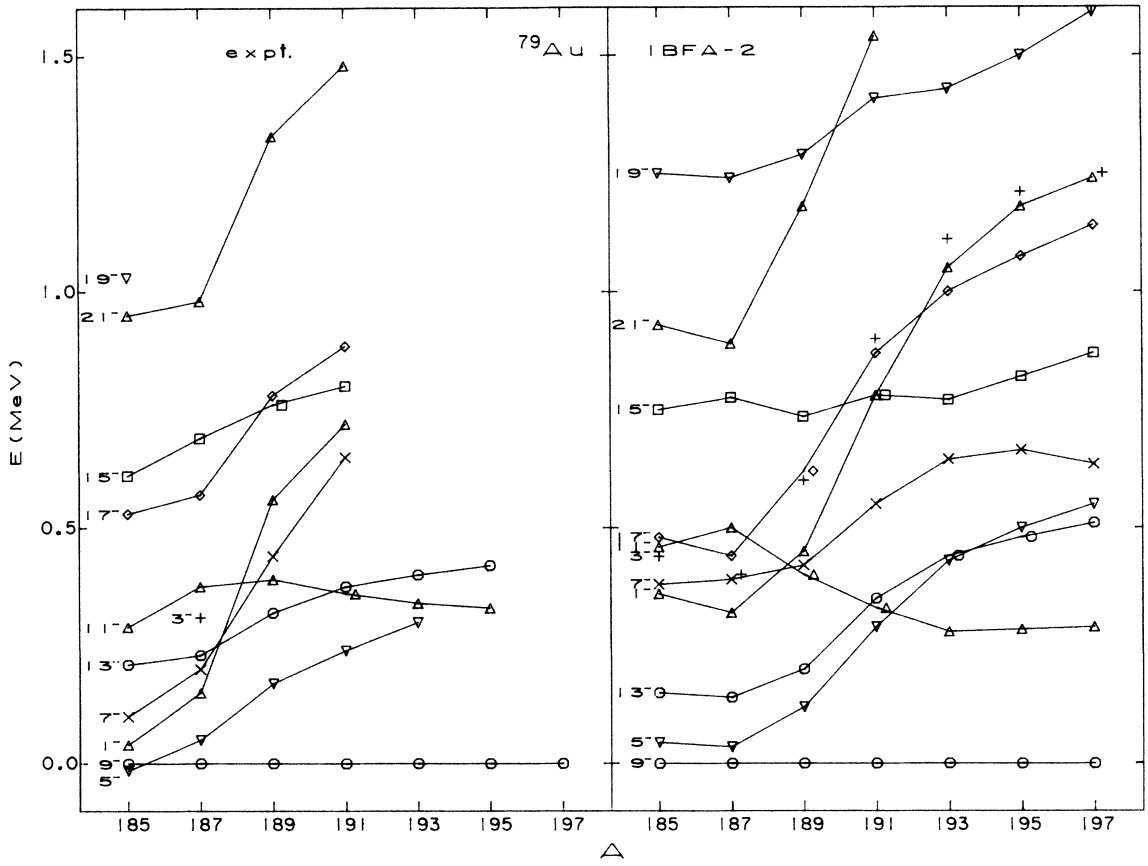

FIG. 11. Experimental (Refs. 43—45) and IBFA-2 systematics of the $\pi h_{9/2}$ band in Au isotopes. The state $J^p=\frac{9}{2}^-$ is taken as zero of energy. Numbers at the left of the curves are twice the spin of the level.

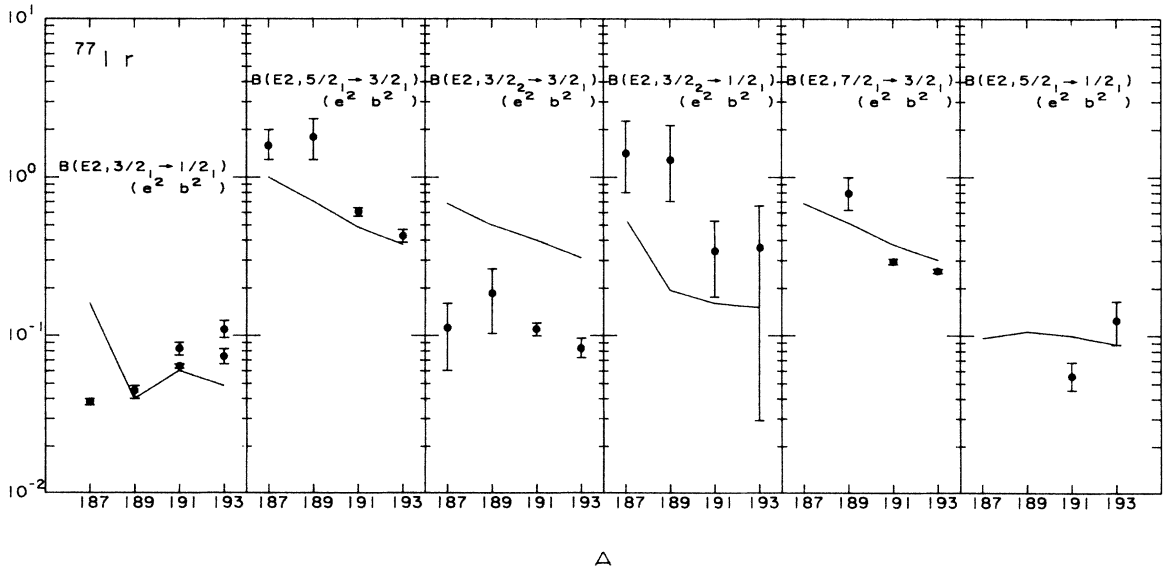

FIG. 12. Experimental (Refs. 37 and 47—50) and calculated $B(E2)$'s in some positive parity states in Ir isotopes.

TABLE VI. Comparison between calculated and experimental $B(M1)$ values (in μ_N^2) for $^{187-193}$Ir. The experimental data are taken from Refs. 37, 47, and 49.

$J_i^\pi \to J_f^\pi$	Nucleus	Expt.	IBFA-2	Nucleus	Expt.	IBFA-2
$\frac{3}{2}^+_1 \to \frac{1}{2}^+_1$	^{187}Ir	$<3.1\times10^{-6}$	0.002	^{189}Ir	0.000 016(3)	0.000 009
$\frac{5}{2}^+_1 \to \frac{3}{2}^+_1$		0.032(4)	0.009		0.054(12)	0.000 16
$\frac{3}{2}^+_2 \to \frac{3}{2}^+_1$		0.0067(30)	0.001		0.0048(22)	0.001
$\frac{5}{2}^+_2 \to \frac{3}{2}^+_2$		0.55(11)	0.073		0.42(14)	0.012
$\frac{7}{2}^+_1 \to \frac{5}{2}^+_1$			0.013		0.100(20)	0.016
$\frac{3}{2}^+_1 \to \frac{1}{2}^+_1$	^{191}Ir	0.000 43(1)	0.000 016	^{193}Ir	0.000 63(6)	0.000 03
$\frac{5}{2}^+_1 \to \frac{3}{2}^+_1$		0.0328(31)	0.005		0.058(11)	0.005
$\frac{3}{2}^+_2 \to \frac{3}{2}^+_1$		0.0029(6)	0.003		0.0048(29)	0.003
$\frac{5}{2}^+_2 \to \frac{3}{2}^+_2$		0.106(16)	0.085		0.109(13)	0.128
$\frac{7}{2}^+_1 \to \frac{5}{2}^+_1$		0.054(20)	0.025		0.054(20)	0.022

for $(s_{1/2}\times0_1^+)^{1/2}$ in the $\frac{1}{2}^+$ state a probability of about 80%, about 8% of $(d_{3/2}\times2_1^+)^{1/2}$, and 9% and 5% of $(d_{3/2}\times2_2^+)^{1/2}$ for ^{191}Ir and ^{193}Ir, respectively. The experimental data have been taken from Refs. 35, 37, 47, 48, and 51.

The discrepancy between $\mu_{\text{expt}}(\frac{3}{2}^+_2)$ and $\mu_{\text{theo}}(\frac{3}{2}^+_2)$ seems to be due to the fact that the calculated $\frac{3}{2}^+_2$ does not correspond to the experimental one. Figure 12 supports this idea. The differences in the other magnetic moments may arise from the fact that they are very sensitive to the choice of the single particle orbits (ordering and spacing). Another important point is the quenching of $g_{s_\pi}^{\text{free}}$, since it enters the single particle part of the $M1$ operator. If we used a quenching of $g_{s_\pi}=0.9g_{s_\pi}^{\text{free}}$, we would get $\mu(\frac{3}{2}^+_1)=+0.181\ \mu_N$ $(+0.213\ \mu_N)$ and $\mu(\frac{1}{2}^+_1)=+2.045\ \mu_N$ $(+2.150\ \mu_N)$ for ^{191}Ir (^{193}Ir). Then, the smaller quenching of $g_{s_\pi}=0.9g_{s_\pi}^{\text{free}}$ seems to account better for the magnetic moment of the ground state. However, $\mu(\frac{1}{2}^+_1)$ is still overestimated because of the large $s_{1/2}$ component. This may be avoided by raising the $s_{1/2}$ single particle orbit. As a conclusion, we can say that a more precise knowledge of the single particle orbits is crucial in order to study the $M1$ properties in odd-even nuclei.

An additional test of the wave functions could be made by comparing the spectroscopic factors for one nucleon transfer. Work in this direction is in progress.

TABLE VII. Calculated and experimental magnetic moments (in μ_N) for ^{191}Ir and ^{193}Ir.

Nucleus	J^π	Expt.	IBFA-2
^{191}Ir	$\frac{3}{2}^+_1$	$+0.146(1)^{d}$	0.454
	$\frac{1}{2}^+_1$	$+0.542(5)^{c}$	1.555
	$\frac{5}{2}^+_1$	$+0.62(7)^{d}$	1.097
	$\frac{3}{2}^+_2$	$+1.40(38)^{a}$	−0.123
^{193}Ir	$\frac{3}{2}^+_1$	$+0.163(6)^{a}$	0.501
	$\frac{1}{2}^+_1$	$+0.504(3)^{a}$	1.628
	$\frac{5}{2}^+_1$	$+0.73(13)^{a}$	1.143
	$\frac{3}{2}^+_2$	$+1.02(38)^{b}$	−0.112

[a]Reference 35.
[b]Reference 48.
[c]Reference 37.
[d]References 47 and 51.

D. Negative parity states

We present in Table VIII some experimental data for $E2$ and $M1$ transitions, moments, and mixing ratios found in the literature[33,54] on negative parity states along with their corresponding calculated values. The parameters used are those given for positive parity states. The good agreement for these negative parity states is remarkable. It is worth noticing that the composition of the wave functions of the $\frac{7}{2}^-_1$ and $\frac{11}{2}^-_1$ states in ^{191}Ir is mainly $(\frac{11}{2}^-\times2_1^+)$ (58%) and $(\frac{11}{2}^-\times2_2^+)$ (32%) for the $\frac{7}{2}^-_1$ and $(\frac{11}{2}^-\times0_1^+)$ (54%) and $(\frac{11}{2}^-\times2_1^+)$ (40%) for the $\frac{11}{2}^-_1$, yielding a value of the $B(E2;\frac{7}{2}^-_1\to\frac{11}{2}^-_1)$ in agreement with the experimental data. This represents a more complex situation than those discussed in Ref. 54.

V. CONCLUDING REMARKS

We have presented in this paper a complete set of calculations of the odd-proton ($_{77}$Ir,$_{79}$Au) and the odd-neutron ($_{78}$Pt) isotropic chains within the framework of the proton-neutron interacting boson-fermion model. Single j calculations have been performed to describe those bands built mainly on a single j shell with high spin, and in order to describe configurations in which several single-particle levels are involved we have done multilevel calcu-

TABLE VIII. Electromagnetic properties of the $h_{11/2}$ band in ^{187}Ir and ^{191}Ir. The experimental data are taken from Refs. 33 and 34.

Nucleus	Property	Expt.	IBFA-2
^{187}Ir	$\frac{B(E2;\frac{15}{2}_1\rightarrow\frac{11}{2}_1)}{B(E2;\frac{15}{2}_1\rightarrow\frac{13}{2}_1)}$	$1.7^{+\infty}_{-1.4}$	0.4
	$\frac{B(E2;\frac{17}{2}_1\rightarrow\frac{13}{2}_1)}{B(E2;\frac{17}{2}_1\rightarrow\frac{15}{2}_1)}$	$0.8^{+0.2}_{-0.6}$	0.6
	$\frac{B(E2;\frac{15}{2}_2\rightarrow\frac{11}{2}_1)}{B(E2;\frac{15}{2}_2\rightarrow\frac{13}{2}_1)}$	<0.1	0.09
	$\delta(E2/M1)(\frac{9}{2}_1\rightarrow\frac{11}{2}_1)$	$-0.4<\delta<-0.15$	-0.182
	$\delta(E2/M1)(\frac{13}{2}_1\rightarrow\frac{11}{2}_1)$	0.25—0.40	0.323
	$\delta(E2/M1)(\frac{17}{2}_1\rightarrow\frac{15}{2}_1)$	0.15—0.25	0.256
	$\delta(E2/M1)(\frac{15}{2}_2\rightarrow\frac{13}{2}_1)$	$\delta>0.28$	0.735
	$\delta(E2/M1)(\frac{15}{2}_1\rightarrow\frac{13}{2}_1)$	0.0—0.25	0.203
^{191}Ir	$B(E2;\frac{7}{2}_1\rightarrow\frac{11}{2}_1)$	0.37 ± 0.04 e^2b^2	0.405 e^2b^2
	$\mu(\frac{11}{2}_1)$	3.27 ± 0.12 μ_N	6.68 μ_N
		6.026 ± 0.036 μ_N	
	$\delta(E2/M1)(\frac{17}{2}_1\rightarrow\frac{15}{2}_1)$	0.10—0.30	0.486
	$\delta(E2/M1)(\frac{9}{2}_1\rightarrow\frac{7}{2}_1)$	0.20—0.50	0.045
	$\delta(E2/M1)(\frac{11}{2}_2\rightarrow\frac{9}{2}_1)$	0.2—0.5	0.15
	$\delta(E2/M1)(\frac{21}{2}_1\rightarrow\frac{19}{2}_1)$	$\lvert\delta\rvert<0.05$	0.592

lations. It has been shown that the proton-neutron IBFA is able to describe the main features of the energy spectra of these isotopic chains accounting for the transition from O(6)-plus-particle to SU(3)-plus-particle limits of IBFA. With the present parametrization only three parameters are needed to describe a complete chain and these are fixed or vary smoothly.

These calculations where proton and neutron degrees of freedom are treated explicitly seem to confirm the general feeling that the quadrupole-quadrupole force between the odd neutron (proton) and the core nucleus is dominated by the quadrupole-quadrupole interaction of the odd neutron (proton) and the protons (neutrons) in the core nucleus.

This work shows that entire regions of the *Table of Nuclides* can be correlated within the relatively simple framework of IBFA-2. Due to the previously mentioned behavior of the parameters needed in this model, it is a straightforward task to extrapolate the calculations towards nuclear regions not yet experimentally studied and to make predictions on properties hitherto unknown.

In general, electromagnetic properties are poorly reproduced by the IBFA-2 calculations. Some IBFA-2 calculations have already been carried out in the transitional region SU(5)→SU(3) (Xe-Cs).[22,52,55] In order to complete this study to check the scope and limitations of the model, calculations in the transitional region O(6)→SU(5) (Pd-Rh) are in progress.

ACKNOWLEDGMENTS

We are indebted to Prof. F. Iachello for calling our attention to this study, to Prof. G. Madurga for his comments and critical reading of the manuscript, and Dr. R. Bijker for providing us with the computer codes. This work was supported in part by the Spanish Comisión Asesora de Investigación Científicia y Técnica, Contract No. 2868-83.

[1]M. Piiparinen, J. C. Cunnane, P. J. Daly, C. L. Dors, F. M. Bernthal, and T. L. Khoo, Phys. Rev. Lett. **34**, 1110 (1975).

[2]T. L. Khoo, F. M. Bernthal, C. L. Dors, M. Piiparinen, S. K. Saha, P. J. Daly, and J. Meyer-ter-Vehn, Phys. Lett. **60B**, 341 (1976).

[3]S. K. Saha, M. Piiparinen, J. C. Cunnane, P. J. Daly, C. L. Dors, T. L. Khoo, and F. M. Bernthal, Phys. Rev. C **15**, 94 (1977).

[4]G. R. Smith, N. J. Di Giacomo, M. L. Munger, and R. J. Peterson, Nucl. Phys. **A290**, 72 (1977).

[5]G. Berrier-Ronsin, M. Vergnes, G. Rotbard, J. Vernotte, J. Kalifa, R. Seltz, and H. L. Sharma, Phys. Rev. C **17**, 529

(1978).
[6]C. Schück, J. Genevey-Rivier, V. Berg, A. Knipper, G. Walter, C. Richard-Serre, and A. Höglund, Nucl. Phys. **A325**, 421 (1979).
[7]S. André, J. Genevey-Rivier, J. Treherne, R. Kaczarowski, J. Łukasiak, J. Jastrzebski, and C. Schück, Nucl. Phys. **A325**, 445 (1979).
[8]G. Rotbard, G. Berrier-Ronsin, M. Vergnes, J. Kalifa, J. Vernotte, and R. J. Sheline, Phys. Rev. C **21**, 1232 (1980).
[9]A. Bohr, K. Dan. Vidensk. Selsk., Mat.-Fys. Medd. **26**, No. 14 (1952).
[10]J. Meyer-ter-Vehn, Nucl. Phys. **A249**, 111 (1975); **A249**, 141 (1975).
[11]H. Toki and A. Faessler, Nucl. Phys. **A253**, 231 (1975).
[12]G. Leander, Nucl. Phys. **A273**, 286 (1976).
[13]F. Iachello and O. Scholten, Phys. Rev. Lett. **43**, 679 (1979).
[14]A. Arima and F. Iachello, Phys. Rev. Lett. **35**, 1069 (1975).
[15]A. Arima and F. Iachello, Ann. Phys. (N.Y.) **99**, 253 (1976); **111**, 201 (1978); **123**, 468 (1979).
[16]For a review see, *Interacting Bosons in Nuclear Physics,* edited by F. Iachello (Plenum, New York, 1979).
[17]R. Bijker and A. E. L. Dieperink, Nucl. Phys. **A379**, 221 (1982).
[18]U. Kaup, A. Gelberg, P. von Brentano, and O. Scholten, Phys. Rev. C **22**, 1738 (1980).
[19]O. Scholten, Ph.D. thesis, University of Groningen, 1980.
[20]O. Scholten and N. Blasi, Nucl. Phys. **A380**, 509 (1982).
[21]M. A. Cunningham, Nucl. Phys. **A385**, 204 (1982); **A385**, 221 (1982).
[22]C. E. Alonso, J. M. Arias, R. Bijker, and F. Iachello, Phys. Lett. **144B**, 141 (1984).
[23]V. Visscher and R. Bijker, Computer Program ODDPAR, 1983, Kernfysisch Versneller Instituut, Groningen.
[24]A. Arima, T. Otsuka, F. Iachello, and I. Talmi, Phys. Lett. **66B**, 205 (1977); T. Otsuka, A. Arima, F. Iachello, and I. Talmi, *ibid.* **76B**, 139 (1978).
[25]O. Scholten and A. E. L. Dieperink, in *Interacting Bose-Fermi Systems in Nuclei,* edited by F. Iachello (Plenum, New York, 1981), p. 343.
[26]I. Talmi, in *Interacting Bose-Fermi Systems in Nuclei,* edited by F. Iachello (Plenum, New York, 1981), p. 329.
[27]R. Bijker, A. E. L. Dieperink, O. Scholten, and R. Spanhoff, Nucl. Phys. **A344**, 207 (1980).
[28]G. Puddu, O. Scholten, and T. Otsuka, Nucl. Phys. **A348**, 109 (1980).
[29]I. Talmi, Nucl. Phys. **A172**, 1 (1972).
[30]T. Otsuka and A. Arima, Phys. Lett. **77B**, 1 (1978).
[31]T. Otsuka, Ph.D. thesis, University of Tokyo, 1979.
[32]T. Otsuka, A. Arima, and F. Iachello, Nucl. Phys. **A309**, 1 (1978).
[33]S. André, J. Boutet, J. Rivier, J. Treherne, J. Jastrzębski, J. Łukasiak, Z. Sujkowski, and C. Sebille-Schück, Nucl. Phys. **A243**, 229 (1975).
[34]J. Łukasiak, R. Kaczarowksi, J. Jastrzębski, S. André, and J. Treherne, Nucl. Phys. **A313**, 191 (1979).
[35]*Tables of Isotopes,* 7th ed., edited by C. M. Lederer and V. S. Shirley (Wiley, New York, 1977).
[36]S. André, J. Genevey-Rivier, J. Treherne, J. Jastrzębski, R. Kaczarowski, and J. Łukasiak, Phys. Rev. Lett. **38**, 327 (1977).
[37]C. Sebille-Schück, M. Finger, F. Foucher, J. P. Husson, J. Jastrzębski, V. Berg, S. G. Malmskog, G. Astner, B. R. Erdal, P. Patzelt, and P. Siffert, Nucl. Phys. **A212**, 45 (1973); A. Bäcklin, G. Hedin, V. Berg, and S. G. Malmskog, *ibid.* **A181**, 76 (1972); S. G. Malmskog, V. Berg, A. Bäcklin, and G. Hedin, *ibid.* **A143**, 160 (1970); V. Berg, S. G. Malmskog, and A. Bäcklin, *ibid.* **A143**, 177 (1970).
[38]J. A. Cizewski, D. G. Burke, E. R. Flynn, R. E. Brown, and J. W. Sunier, Phys. Rev. C **27**, 1040 (1983).
[39]M. Piiparinen, S. K. Saha, P. J. Daly, T. L. Khoo, C. L. Dors, and F. M. Bernthal, Nucl. Phys. **A265**, 253 (1976).
[40]P. J. Daly, C. L. Dors, H. Helppi, M. Piiparinen, S. K. Saha, F. M. Bernthal, and T. L. Khoo, Michigan State University Cyclotron Laboratory Annual Report, 1977—78.
[41]D. D. Warner, R. F. Casten, M. L. Stelts, H. G. Borner, and G. Barreau, Phys. Rev. C **26**, 1921 (1982).
[42]Y. Yamazaki and R. K. Sheline, Phys. Rev. C **14**, 531 (1976).
[43]E. F. Zgankar, *Proceedings of the International Symposium on Future Directions in Studies of Nuclei Far From Stability, Nashville, Tennessee, 1979,* edited by J. H. Hamilton *et al.* (North-Holland, Amsterdam, 1980), p. 49.
[44]M. G. Desthuilliers, C. Bourgeois, P. Kilcher, J. Letessier, F. Beck, T. Byrski, and A. Knipper, Nucl. Phys. **A313**, 221 (1979).
[45]C. Bourgeois, P. Kilcher, J. Letessier, V. Berg, M. G. Desthuilliers, and the ISOCELE collaboration, Nucl. Phys. **A295**, 424 (1978).
[46]M. Sambataro, O. Scholten, A. E. L. Dieperink, and G. Piccito, Nucl. Phys. **A423**, 333 (1984).
[47]C. H. Vieu, S. E. Larsson, G. Leander, I. Ragnarsson, W. de Wieclawik, and J. S. Dionisio, Z. Phys. A **290**, 301 (1979).
[48]H. H. Ghaleb and K. S. Krane, Nucl. Phys. **A426**, 20 (1984).
[49]S. J. Mundy, J. Łukasiak, and W. R. Phillips, Nucl. Phys. **A426**, 144 (1984).
[50]R. Sahu, M. Satpathy, and L. Satpathy, Phys. Rev. C **23**, 1777 (1980).
[51]E. Browne, Nucl. Data Sheets **30**, 653 (1980).
[52]R. Bijker, Ph.D. thesis, University of Groningen, 1984.
[53]P. Kemnitz, L. Funke, H. Sodan, E. Will, and G. Winter, Nucl. Phys. **A245**, 221 (1975).
[54]A. Bäcklin, V. Berg, and S. G. Malmskog, Nucl. Phys. **A156**, 647 (1970).
[55]J. M. Arias, C. E. Alonso, and R. Bijker, Nucl. Phys. **A445**, 333 (1985).